A Comprehensive Approach to Trans-Radial Prosthetic Wearable Technology

Contents

1. Overview

This article proposes an affordable upper limb prosthetic solution to make amputees' lives easier. It includes a comprehensive global market assessment, identifies the target audience, and suggests a plausible solution through benchmarking, feasibility analysis, and concept design. The article focuses on devising a machine learning-based gesture recognition strategy and methods to integrate it into an embedded system. A data pipeline coupled with an ML classifier was developed, which could then be ported to C++, compatible with the proposed system. Furthermore, it evaluates the business profitability and sustainability of the solution.

2. Market Analysis

2.1. Global market outlook

The limb prosthetics market was valued at USD 1.53 billion in 2021 and is estimated to reach USD 2.33 billion by 2029 (Fortune Business Insights, 2022). The main reason for this market growth is the rising number of amputations. The leading players are increasingly transitioning from conventional prostheses to functional ones that use myoelectric and brain-controlled technologies. Despite the strong demand, the high cost of prosthetic devices remains a significant limiting factor. The lower limb segment, which accounts for most global amputations, holds a significant market share.

On the other hand, the upper limb prosthetics market, valued at USD 720 million in 2021, is projected to expand at a CAGR of 5.5% through 2030 (AMR, 2021). Key market players include Ossur, Ottobock SE & Co. KGaA, Steeper Inc., Open Bionics Ltd, CPOUSA, and Coapt LLC. Nonetheless, the US FDA's stringent regulatory compliances and extensive approval procedures may hamper the market's expansion. The primary reason for upper limb loss among adults is trauma, followed by cancer. Other reasons include infections, burns, and congenital deformities. Among upper extremity amputation levels, trans-radial amputation is the most common (47%). The product portfolio includes prosthetic arms, shoulders, wrists, terminal devices, and elbows, catering to end users such as prosthetic clinics and ambulatory surgical centres. Market players focus on developing lightweight and durable prosthetics to meet users' needs; One example is Ossur's Rebound Post-Op Elbow Brace, which launched in July 2021 (AMR, 2021).

Fig. 1. Upper limb prosthetics market trend: www.strategicmarketresearch.com

Recent trends include new polymer materials and 3D printing technology. North America and Europe lead the global market, with the US showing the highest growth potential due to advancing technologies and amputee acceptance. Asia, home to 60% of the world's diabetics, will drive prosthetic demand as diabetes cases rise. The number of Indian diabetes patients aged 20-79 is projected to reach 124.8 million by 2045, leading to a demand surge despite declining amputation rates (GVR, 2022).

2.2. Competitor Analysis

Table.1 showcases some of the latest products in upper limb prosthetics and their characteristics. These details were obtained from the manufacturer websites.

Table. 1 A Comparison of benchmarks

Product	Company	DOF	Sizes (height in mm)	Weight (g)	Number of patterns	Price (USD)
Bebionic Hand	Ottobock	6	S (165) M (190) L (200)	S (390) M (600)	14	11,000 – 20,000
Hero Arm	Open Bionics	5-6	*	S (280) L (346)	6	6,600
LUKE arm	Mobius Bionics	6	S (182.5) M (185.1)	S (507) M (515)	24	Starting at 33,000
i-limb ultra revolution	Ossur	6	316	1400	6	100,000
Michelangelo Hand with Axon Rotation	Ottobock	4	*	450	7	60,000
TASKA' Hand	TASKA prosthetics	8	*	*	23	35,000
VINCENT Evolution 3	Vincent Systems	6	XS (145) S (150) M (160) L (170) XL (180)	XS (386)	14	*
Psyonic Ability Hand	Psyonic	6	S (160) M (210)	S (400) M (450)	6	Starting at 50,000
i-digits quantum	Touch Bionics	5	S (168) L (215)	S (240) L (292)	24	Starting at 50,000

The Hero Arm by Open Bionics is an affordable and customisable prosthetic designed for a range of users, including children and those with limited financial resources or insurance coverage (Open Bionics, n.d.). Its 3D printing technology reduces manufacturing costs while allowing for personalised adjustments. The Michelangelo Hand with Axon Rotation offers integrated wrist functionality, including passive flexion and passive/active rotation. Its electrically controlled axon rotation enables bi-manual activities using myosignals. Notably, all actuators are controlled by a single drive.

Ossur's i-limb ultra revolution features individually motorised digits with a compliant grip and stall-out ability (ossur.com, n.d.). Its electronically rotatable thumb switches between lateral and oppositional positions. The prosthetic's speed boost option reduces response time by 30%. Its mobile app allows access to programmable grip patterns through Quick Grips™ with a simple tap.

2.3. Proposal Overview

The proposed solution is intended for Asian markets considering their growth potential. The high cost of these products is a major barrier to their adoption. The material used for the prosthetic components is the key contributor to the price. A potential solution is to use 3D printing technology, as demonstrated by open bionics and Otto bock. This approach could reduce the material costs and increase the accessibility of upper limb prostheses. The product is to be developed as a mass producible trans-radial prosthetic device. Section 3 investigates some cost-effective choices of hardware and software, based on some market benchmarks.

3. Technical Feasibility Analysis

3.1. Hardware

The main components of a trans-radial prosthetic arm are the microcontroller, actuators, sensors, battery, and the prosthetic component.

3.1.1. Microcontroller:

A variety of microcontrollers are used in wearable technology applications; Their specifications are tabulated below. The desirable solution is a low-power microcontroller that can interface with myoelectric and IMU sensors to trigger actuators to move accordingly.

Table. 2. A Comparison of compatible microcontrollers for prosthetic arms

Series (Make)	Processor	Price	Flash memory	RAM	Clock speed	Peripherals	GIOP pins	Voltage (Max Current)
Atmel SAMD21 (Atmel)	ARM Cortex-M0+ (32 bit)	$1.50 to $3.00	32 KB to 256 MB	32 KB	Up to 48 MHz	USB port, I2C bus, UART, CAN bus, 12-bit ADC	14-64	1.8V to 3.6V (100mA)
Nordic nRF52832 (Nordic Semiconductor)	ARM Cortex-M4 (32-bit)	$2.50 to $5.00	64 KB to 512 KB	128 KB to 512 KB	Up to 64 MHz	USB port, I2C bus, UART, SPI bus, Bluetooth Low Energy, 12-bit ADC	32-64	1.7V to 3.6V (100 mA)
Espressif ESP32(Espressif Systems)	Xtensa LX6 dual core (32-bit)	$3.00 to $10.00	512 KB to 16 MB	128 KB to 520 KB	Up to 240 MHz	2x 100 Mbps Ethernet, Wi-Fi, Bluetooth Low Energy, USB host/device, I2C bus, UART, SPI bus, 12-bit ADC	32-54	3.3V (80 mA)
TI MSp430F5529 (Texas Instruments)	RISC processor (16-bit)	$1.00 to $2.00	256 KB	10 KB	16 MHz	PWM, I2C bus, UART, SPI bus, 10-bit ADC	24-51	1.8V to 3.6V (10 mA)
Kinetis MK22 (NXP)	ARM Cortex-M4 (32-bit)	$1.50 to $3.00	128 KB to 1 MB	64 KB to 128 KB	Up to 120 MHz	FPU, SIMD, DSP, I2C bus, UART, SPI bus, 12-bit ADC	34-64	1.8V to 3.6V (20mA)

The higher the clock speed of a processor, the better it will be to attain higher sampling rates from sEMG electrodes. For our application, the sampling rate is 1 KHz. 16-256 KB of RAM would be sufficient for pattern recognition purpose. Moreover, power consumption, size, weight, and cost are important factors for choosing a microprocessor for wearable technology.

The MK22 from NXP is a 32-bit microcontroller used in the Thalmic MYO armband for gesture recognition (adafruit.com, 2016). It has a built-in ADC, making it suitable for DSP applications. It communicates with an nRF52822 chip for Bluetooth functionality and receives inputs from an InvenSense MPU-9150 9-axis kinematic fusion sensor. Open Bionics employs the TI MSP430F5529 microcontroller in their Hero Arm (Open Bionics, n.d.). The microcontroller handles eight sEMG signals for gesture recognition and controls four actuators. It communicates with an nRF52822, like the MK22 in the MYO armband.

The Espressif ESP32 is a new and powerful microcontroller option with a dual-core 32-bit Xtensa LX6 processor, ample memory, built-in Wi-Fi and Bluetooth connectivity (futureelectronics.com, n.d.). It provides more processing power than other microcontrollers like Atmel SAMD21 and Nordic nRF52832. The ESP32's price varies but generally falls within the $5 to $10 range, making it a cost-effective choice for developers seeking versatility.

Given below is a tabulation of the programming languages supported by each microcontroller.

Table. 3. Microcontrollers and the programming languages they support

Processor	Programming language
Atmel SAMD21	Arduino IDE (C/C++), MicroPython
Nordic nRF52832	Arduino IDE (C/C++), nRF Connect SDK (C/C++), Zephyr (C/C++), MicroPython
Espressif ESP32	Arduino IDE (C/C++), Espressif IDF (C/C++), MicroPython
TI MSP430F5529	IAR Embedded Workbench for MSP430 (C), Energia IDE (C/C++)
Kinetis MK22FNM0V12	Keil uVision IDE (C/C++), IAR Embedded Workbench for ARM (C/C++)

3.1.2. Actuators:

Actuators are the devices that power the movements of prosthetic arms. They come in various types, each with its advantages and disadvantages. Electric motors are the most common type of actuator used in prosthetic arms. They are robust and reliable, and they can be controlled with a high degree of precision. However, they can be bulky and heavy.

Other types of actuators such as shape memory alloy (SMA), hydraulic, and pneumatic actuators are also used in prosthetics, though uncommon since they are difficult to control. SMA actuators are made of materials such as nickel-titanium (NiTi), copper-aluminium-nickel (CuAlNi); They change shape when heated. They are lightweight and compact but cannot deliver high torque. On the other hand, pneumatic and hydraulic actuators offer more torque than electric motors. Choice on the number of actuators depend on the functionality of the prosthetic arm. This can include basic features such as hand opening and closing, wrist rotation etc to more complex functionalities such as controlling individual fingers.

Table. 4. Actuators used in benchmark arms and their functions

Product	Number of Actuators	Functions
Bebionic Hand	6	F1, F2
Hero Arm	4	F2, F3, F4, F5
LUKE arm	4	F9, F10, F2, F3
i-limb ultra revolution	6	
Michelangelo Hand with Axon Rotation	4	F11, F5, F6, F7
TASKA' Hand	5	F11, F5, F6, F7, F8
VINCENT Evolution 3	4	F9, F10, F2, F3
Psyonic Ability Hand	5	F11, F5, F6, F7, F8
i-digits quantum	5	F11, F5, F6, F7, F8

Table. 5. Description of functions in Table. 4

Function	Description
F1	One for each finger joint
F2	Wrist rotation
F3	Hand opening and closing
F4	Thumb rotation
F5	Index finger flexion and extension
F6	Middle finger flexion and extension
F7	Ring finger flexion and extension
F8	Pinky finger flexion and extension
F9	Shoulder flexion and extension
F10	Elbow flexion and extension
F11	Thumb opposition

3.1.3. Sensors:

In addition to surface electromyography (sEMG) sensors, which are used to measure the electrical activity of muscles, other important sensors used in prosthetic arms include position, force, touch, and temperature sensors. Force sensors monitor the kinematics of the prosthetic components and, along with position sensors, act as a feedback system for the microcontroller to drive the arm as desired. In the MYO armband, the main Kinetis microcontroller is coupled with the InvenSense MPU 9150, which acquires triaxial magnetic field strength, angular velocity, and acceleration data; This methodology can be adopted for prosthetic arms as well.

Another common type of sensor used in prosthetics is the pressure sensor. For example, the Hero Arm and i-limb ultra revolution both have a series of pressure sensors on the fingertips that indirectly measure the contact force when gripping objects; This can help the microcontroller to signal the actuators to attain an optimal grip force. Products such as the i-Limb Quantum and Michelangelo Hand use temperature sensors to provide feedback to the user about the temperature of objects that the hand interacts with, as a safety measure.

3.1.4. Proposed Hardware Solution:

The proposed system is composed of the following components:

- **Microprocessor:** A 32-bit Kinetis MK22 processor with an ARM M-4 Cortex architecture provides the computational power and control for the system. The processor has an operating voltage of 1.7 V to 3.6 V, and supports sensors with a maximum voltage of 3.3 V.
- **Battery:** The Friwo FB2S1P18650-26 battery, a Li-ion battery with a voltage of 7.5 V and a capacity of 2600 mAh, provides power for the system.
- **sEMG sensors**: Myowave muscle sensors are electromyography (EMG) sensors that acquire electrical signals from the user's muscles. The sensor has a supply voltage requirement of 3.3 V and communicate with the Kinetis MK22 processor through a UART peripheral.
- **Kinematic fusion:** The InvenSense MPU 6050 kinematic fusion sensor is an inertial measurement unit (IMU) that integrates a tri-axial gyroscope and accelerometer. The sensor communicates with the Kinetis MK22 processor through an I2C peripheral. The sensor provides information about the orientation and movement of the arm.
- **Actuators:** Four SMA linear actuators control the joints of the bionic arm.

An estimate of power consumption for each component is required to calculate the battery life. Assuming a nominal voltage of 7.5V,

$$\text{Battery life (hours)} = \frac{\text{Battery capacity(mAh)}}{\left(\text{Total current draw (mA)}\right)}$$

The MK22 processor consumes 3.6mA (run) and 0.9mA (sleep); The average consumption at 50% duty cycle is 2.25mA. Furthermore, the Myowave sensors consume 15mA each; With four sensors, the total consumption is 60mA. The MPU 6050 sensor consumes 3.9mA (normal) and 0.5mA (low power); The average consumption at 50% duty cycle is 2.2mA. Finally, the SMA linear actuators have 1-ohm resistance and operate at 10Hz frequency with a 10% duty cycle; The average consumption is 40 mA each. With four actuators, the total consumption is 160 mA.

Total system current draw:

2.25 mA + 60 mA + 2.2 mA + 160 mA = 224.45 mA

Battery life = $\frac{2600\ \text{mAh}}{224\ \text{mA}}$ = 11.60 hours

Note: This calculation is approximate and does not consider temperature, efficiency, or other factors affecting system performance.

3.2. Software

3.2.1. Control Algorithm:

A control algorithm decodes sEMG signals, recognizes hand gestures, and performs actions. Fig. 2 shows the flowchart of the algorithm. The signal is filtered to remove noise and then processed to compute the RMS using a window size. Downsampling is done with an appropriate window overlap. Feature extraction is performed using PCA to capture maximum data variance. Extracted features are classified using a machine-learning model into six gesture classes: rest, clenched fist, wrist flexion, wrist extension, radial deviation, and ulnar deviation. For the arm actuation, control commands are generated based on the recognized gesture. The microcontroller receives feedback from gyroscopes, accelerometers, temperature, and pressure sensors, providing execution information. Section 4 provides detailed proof of concept.

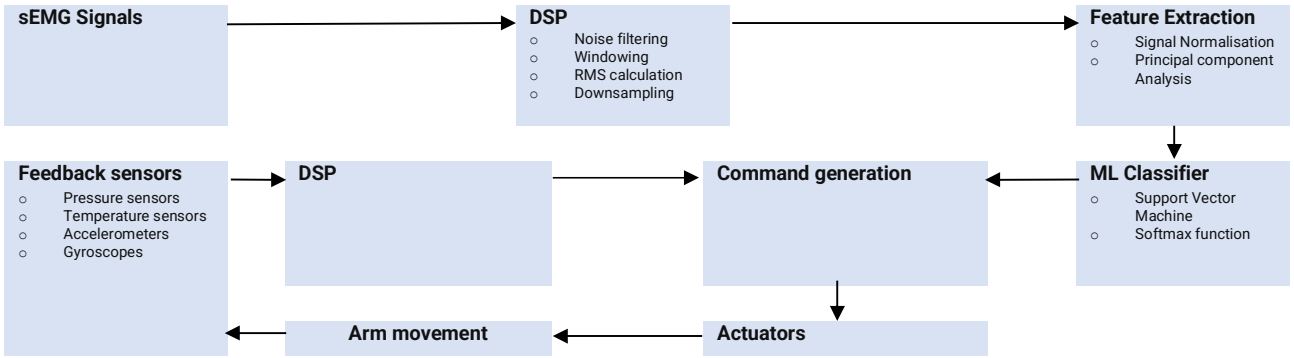

Fig. 2 Schematic of the control algorithm

3.2.2. User Interface:

The proposed bionic arm could incorporate a user interface (UI) based on the Windows operating system, with which it communicates via Bluetooth. The UI would facilitate the calibration of sEMG sensors and signal gain adjustment, allowing customization of the arm control. The Interface could include real-time monitoring of sEMG signals, grip strength, and movement accuracy, enabling users to check for proper functioning. Additionally, a virtual training module could be included to guide the user through the setup process and provide practice sessions.

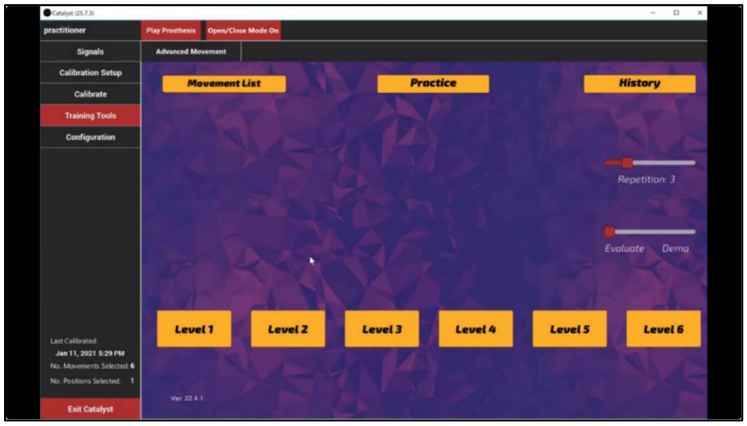

Fig. 3. Catalyst: The UI of Sense system developed by IBT (Infinite Biomedical Technology) (i-biomed.com, n.d.)

4. Proof of Concept

This section explains the data analysis and implementation of an ML framework for gesture recognition. The dataset for this analysis was acquired using a MYO Thalmic bracelet worn by 35 subjects performing seven hand gestures (Table. 6) (UCI ML repository, n.d.). The bracelet receives sEMG signals from eight sensors mounted radially around the forearm. The extended palm gesture was discarded from the analysis due to its insufficient sample count (Fig. 4). Following an Exploratory Data Analysis (EDA), a data pipeline was developed that will do all the necessary pre-processing and feature transformations on any new data that is acquired on a real-time basis. This transformed data could then be fed into a tuned ML model to perform gesture recognition effectively.

Table. 6 Hand gestures considered for the analysis.

Hand gesture	Numeric Label
Hand at rest	1
Hand clenched in a fist	2
Wrist flexion	3
Wrist extension	4
Radial deviation	5
Ulnar deviation	6
Extended palm	7

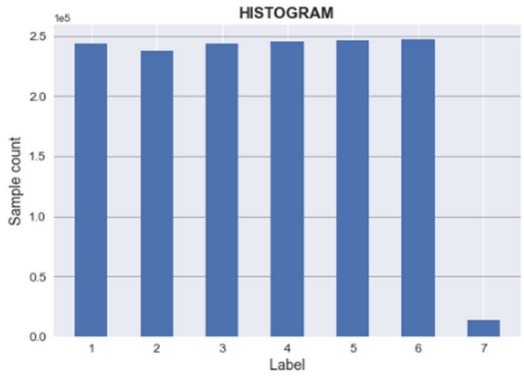

Fig. 4. Histogram of Labels

4.1. Data Pre-processing

For sEMG signals, the frequency range of 50 Hz to 450Hz holds a major portion of the energy and has been proven to be sufficient for ML applications (Wu, Li, Liu, & Wang, 2019). To remove noisy elements from the signal, a band-pass filter is applied within this frequency range. Two critical parameters for gesture recognition are the processing window size and the overlap. While larger window sizes may improve classification accuracy, they come at the cost of increased response time. Conversely, smaller window sizes may result in insufficient data per window for classification. The choice of overlap is dependent on the minimum number of samples that can be skipped without causing a loss of representativeness. For real-time gesture recognition, the window size is typically kept between 50ms to 250ms (Li, Shi, & Yu, 2021). Here, two window sizes, 100ms and 200ms, were investigated.

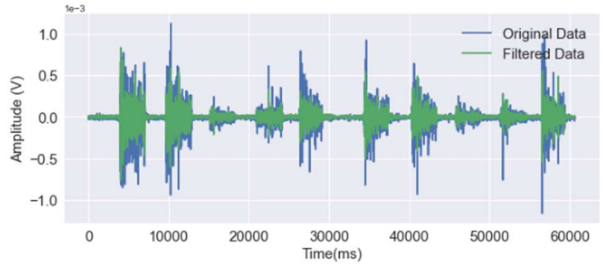

Fig. 5. Applying Band Pass Filter (50-450Hz) to an sEMG signal

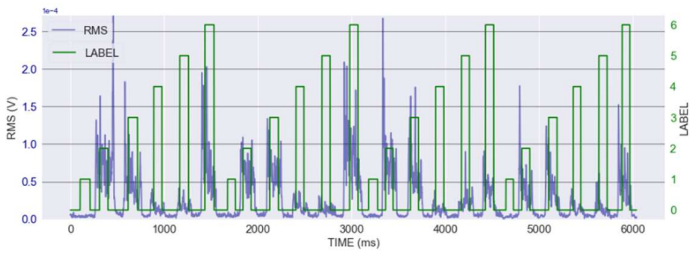

Fig. 6. RMS (100ms window) vs time for an sEMG signal

The autocorrelation function (ACF) is a measure of correlation between a signal and its time-lagged values. This function can detect correlation within the signal. An ACF analysis performed on the sEMG signal showed near zero correlation after 20 lags, implying that one in every 20 consecutive samples could still be representative of the data (Fig. 7). RMS features were extracted from the filtered signal and were downsampled to 50 Hz ($i.e., \frac{1000}{20}\ Hz$).

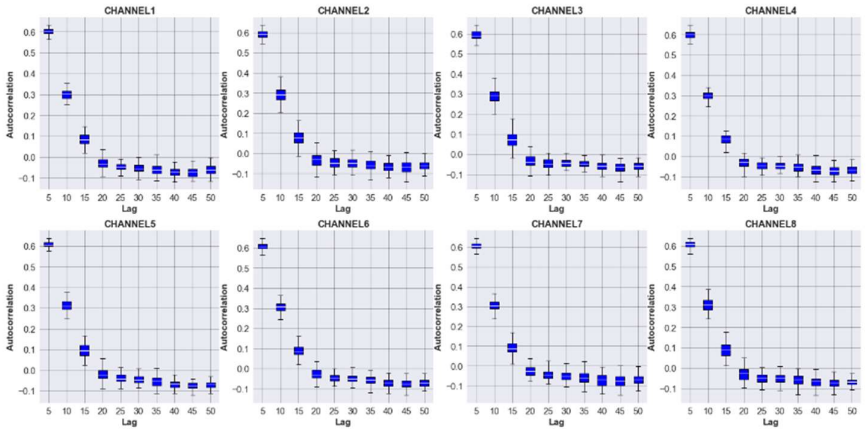

Fig. 7. Autocorrelation vs lag plot for all the sEMG channels

4.2. Feature Extraction

Principal Component Analysis (PCA) is a technique used to transform the feature matrix into the principal component space. The principal axes correspond to the eigenvector directions, along which the data's variance is maximum. PCA enables ML models to identify patterns faster and more efficiently than otherwise. Prior to PCA, RMS signals were normalised by subtracting by the mean and dividing by the standard deviation, which is done to ensure all features are numerically in the same range. First five principal components explain nearly 90% of variance in the data (Fig. 8). Clusters look closely packed when plotted on the first two principal axes (Fig. 9). All the eight principal components were considered for the classification task.

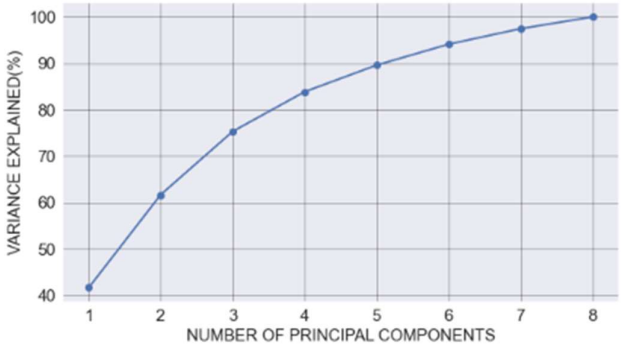

Fig. 8. Variance explained by the first n principal components.

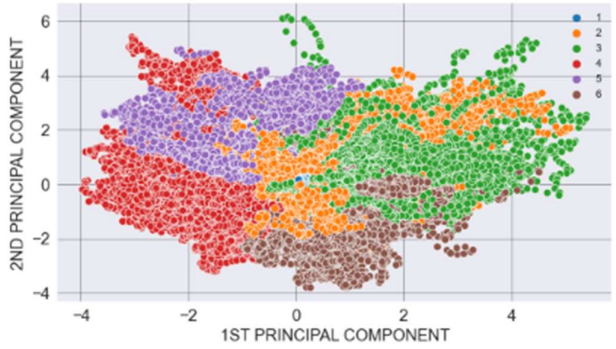

Fig. 9. Orthographic projection of RMS data on the first two principal components

4.3. Performance Measures

Different models were developed and compared with each other for the best performance. Accuracy is chosen as the primary evaluation metric in this work because the dataset is balanced. Other measures used here include precision, recall, and F1-score, with further information provided in Table 7. A confusion matrix is a table that summarises the performance of a classification model on the test data. It shows the number of correct and incorrect recognitions for each gesture, and how the model confuses one class with another. An example confusion matrix with only two outcomes is illustrated in Fig. 10.

Table. 7. Performance measures used in this work

Performance metric	Formula	Definition
Accuracy	$\frac{TP+TN}{TP+TN+FP+FN}$	The proportion of correctly identified gestures in a stream of data
Recall	$\frac{TP}{TP+FN}$	The proportion of correct recognitions for a given type of gesture.
Precision	$\frac{TP}{TP+FP}$	The proportion of correct recognitions among all the recognitions as a certain type of gesture.
F1-Score	$\frac{Recall * Precision}{Recall + Precision}$	The harmonic mean of precision and recall

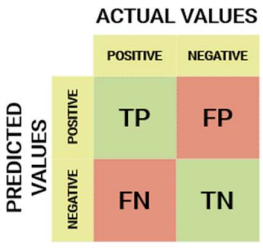

Fig. 10. Structure of a two-by-two confusion matrix

4.4. Classification

A three-stage methodology was adopted for model development and evaluation. Firstly, the 35 subjects were randomly divided into three groups: train, validation, and test sets. Then, hyperparameter tuning was performed, which involves utilising the train set and the validation set to fine-tune

the models for optimal generalisation performance. Once tuned, the models were subsequently deployed to classify the test set data. This study explores the performance of two models, Support Vector Machines and Random Forest Classifiers, for achieving the best classification results.

4.4.1. Support Vector Machine

Support Vector Machines (SVMs) are supervised ML models widely used for performing classification and regression tasks. Being a supervised algorithm, an SVM classifier maps the training examples into a hyperspace such that the separation, or margin, between different classes is maximum. As SVMs are a proven choice for non-linear decision boundaries, they would be suitable for the gesture recognition task as well. To map the feature space into higher dimensions, SVMs use some special functions called kernels. One popular kernel for non-linear classification tasks is the Radial Basis Function (RBF), which is being used here. Two hyperparameters to tune in an RBF-based SVM model are the regularisation parameter, C, and the scale factor, γ. To ensure adaptability with the scale of the features, γ was set as $\frac{1}{variance * N_{features}}$. On the other hand, C was tuned among four values: 0.1, 1, 10 and 100 for the best performance.

The objective function to maximise in an SVM model is,

$$\sum_{i=1}^{n} \propto_i - \frac{1}{2} \sum_{i,j=1}^{n} \alpha_i \alpha_j y_i y_j K(x_i, x_j) \quad ; 0 \leq \alpha_i \leq C$$

where $\propto_i$ is the Lagrange multiplier of X_i.

For an RBF kernel, $K(x_i, x_j) = \exp\left(-\gamma(|x_i - x_j|)^2\right)$.

4.4.2. Random Forest Classifier

A Random Forest Classifier (RFC) is a type of ensemble learning method that uses multiple decision trees to make predictions and is capable of handling both classification and regression problems. RFCs work by randomly selecting subsets of data and features to train different decision trees and then combining their outputs by averaging or voting. This reduces the variance and correlation among the individual trees and improves the generalisation performance of the model. It avoids bias by training decision trees on random data batches; a technique called bootstrap aggregation, or bagging. Number of estimators, or trees, was tuned among 3 values – 50, 100, 200 for the best performance.

4.4.3. Results

The SVM model demonstrates optimal performance at C = 1 for a processing window size of 100ms and at C = 10 for that of 200ms. On the other hand, RFC shows optimal performance with 200 trees, regardless of the window sizes. SVM with a 200ms window exhibits the best performance, achieving a classification accuracy of 88.87 ± 8.19% (Fig. 11). Additionally, it exhibits the highest values for all the performance measures, as presented in Table 8. As anticipated, increasing the window size enhances the accuracy of both models. However, the SVM model shows some confusion between extending palm (6) and wrist flexion (3), as illustrated in the confusion matrix (Fig. 12). Misclassifications between ulnar deviation (5) and wrist extension (4) are also noticeable. Higher performance could be achieved by using a post-processing method such as multi-window joint decision-making, which can correct some window errors using consecutive windows (Li, Shi, & Yu, 2021).

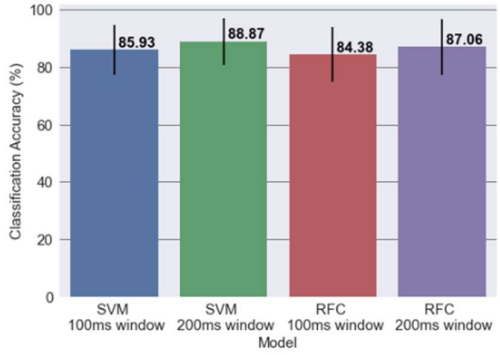

Fig. 11. Classification accuracy of SVM and RFC models with different processing window sizes

Table 8. Performance comparison of SVM and RFC models.

Metric	SVM (100ms window)	SVM (200ms window)	RFC (100ms window)	RFC (200ms window)
Accuracy (%)	85.93	88.87	84.38	87.06
Recall (%)	85.21	88.40	84.27	86.92
Precision (%)	85.44	88.56	85.19	87.28
F1-Score (%)	86.11	89.42	84.76	86.96

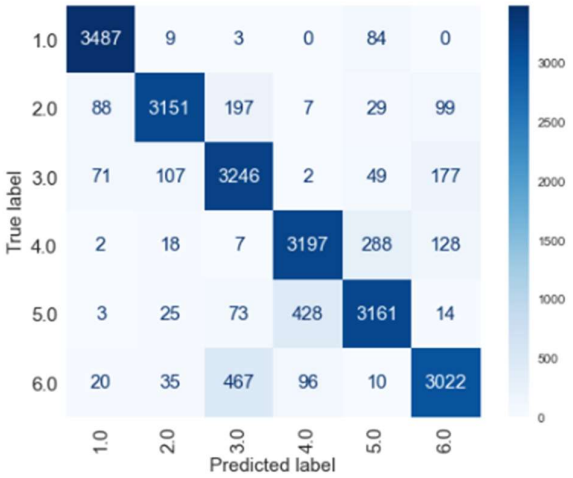

Fig. 12. Confusion matrix for the SVM model (window size = 200ms)

5. Cost analysis

Table.9 provides a rough estimate of the material cost per unit. Fixed cost includes hiring engineers to port the control algorithm to C++, and the Windows-based UI development. Nonetheless, as there exist C++ alternatives to Python libraries used in the classification algorithm developed here, as listed in Table.10, the porting task may be relatively more straightforward. Libraries such as Eigen, Armadillo, and mlpack are designed to

be lightweight and efficient, suitable for embedded systems. They offer linear algebra and numerical computation functionalities, which could be beneficial for tasks like signal processing, machine learning, and PCA. The cost of developing a bionic arm business in the UK is estimated at USD 5 million (gov.uk, 2019); This figure maybe 25% less in Asian markets. Assuming so, if the product is priced at 5000 USD, all the expenses could be covered by selling 1500 units.

Table 9. Performance comparison of SVM and RFC models.

Component	Cost (USD)
3D printed trans-radial arm	2000 $
Microprocessor	3 $
Actuators	50 $
Kinematic fusion	5 $
sEMG sensors	40 x 6 = 240 $
Battery	110 $
Total	2400 $ (approx.)

Table 10. C++ alternatives to python libraries used for the gesture recognition.

Python libraries used	C++ alternatives for embedded systems
NumPy	Eigen, Armadillo, uBLAS, EigenLite
Pandas	RcppDataFrame, TinyCsvParser, FastCSV
Scipy Signal: iift	FFTW, CMSIS-DSP, Armadillo (signal module)
Scipy Signal: butter	C++ implementation required
Scipy Signal lfilter	C++ implementation required
Sklearn PCA	mlpack, Shogun, OpenCV, Armadillo (PCA)

6. Summary

This work aimed to develop an affordable trans-radial prosthetic arm. Market analysis revealed that the Asian market, where diabetic amputation rates are rising, could be the target audience. Following competitor analysis and benchmarking, a plausible hardware solution was developed, accompanied by a corresponding software counterpart. The prosthetic component is intended to be 3D printed.

8-channel, 1 KHz sEMG data from 35 subjects using the MYO Thalmic bracelet was utilised to demonstrate the proof of concept. The signals were denoised using a 50 - 450 Hz bandpass filter. Subsequently, the signal was normalized and transformed using PCA. Two classifiers, SVM and RFC, were employed for the analysis, with SVM exhibiting the best performance. It achieved a mean classification accuracy of 88.87% for 6 gestures. This accuracy can be further improved by implementing suitable post-processing techniques such as Bayesian fusion or joint-window decision-making.

While the analysis was conducted in Python, the availability of C++ alternatives for most libraries allows for a relatively straightforward porting of this solution. Lastly, a cost analysis indicated potential business profitability after selling 1500 products, assuming a unit price of USD 5000.

7. Works Cited

adafruit.com. (2016). *MYO Armband Teardown*. Retrieved from https://learn.adafruit.com/myo-armband-teardown/inside-myo

AMR. (2021). Upper Limb Prosthetics Market by Product Type (Passive Prosthetic Devices, Myoelectric Prosthetic Devices, Body Powered Prosthetic Devices, Hybrid Prosthetic Devices) Component (Prosthetic Wrist, Prosthetic Arm, Prosthetic Elbow, and Prosthetic Shoulder. Retrieved from https://www.alliedmarketresearch.com/upper-limb-prosthetics-market-A12065

Fortune Business Insights. (2022). The global limb prosthetics market is projected to grow from $1.61 billion in 2022 to $2.33 billion by 2029, at a CAGR of 5.4% in the forecast period, 2022-2029... Read More at:- https://www.fortunebusinessinsights.com/limb-prosthetics-market-106893. Retrieved from The global limb prosthetics market is projected to grow from $1.61 billion in 2022 to $2.33 billion by 2029, at a CAGR of 5.4% in the forecast period, 2022-2029... Read More at:- https://www.fortunebusinessinsights.com/limb-prosthetics-market-106893

futureelectronics.com. (n.d.). *Espressif ESP32*. Retrieved from https://www.futureelectronics.com/p/semiconductors--wireless-rf--rf-modules-solutions--wireless-multi-protocol/esp32-wroom-32e-n4-espressif-systems-1157710?msclkid=429c1f6283ae1fa8e6fb7b05db3aeea2&utm_source=bing&utm_medium=cpc&utm_campaign=A-DSA%20PDP%20

gov.uk. (2019). Bionic arm start up secures £4.6 million to go global. Retrieved from https://www.gov.uk/government/news/bionic-arm-start-up-secures-46-million-to-go-global

GVR. (2022). Prosthetics And Orthotics Market Size, Share & Trend Analysis Report By Type ((Orthotics (Upper Limb, Lower Limb, Spinal), Prosthetics (Upper Extremity, Lower Extremity)), By Region, And Segment Forecasts, 2023 - 2030. Retrieved from https://www.grandviewresearch.com/industry-analysis/prosthetics-orthotics-market

i-biomed.com. (n.d.). Retrieved from Infinite Biomedical Technology: https://www.i-biomed.com/sense.html

Li, W., Shi, P., & Yu, H. (2021). Gesture Recognition Using Surface Electromyography and Deep Learning for Prostheses Hand: State-of-the-Art, Challenges, and Future. *Frontiers in Neuroscience*. doi:https://doi.org/10.3389/fnins.2021.621885

Open Bionics. (n.d.). *The Hero Arm*. Retrieved from https://openbionics.com/hero-arm/

ossur.com. (n.d.). *Introduction to i-limb*. Retrieved from ossur.com: https://www.ossur.com/en-us/prosthetics/upper-limb-training/i-limb

UCI ML repository. (n.d.). *EMG dataset*. Retrieved from https://archive.ics.uci.edu/ml/datasets/EMG+data+for+gestures

Wu, J., Li, X., Liu, W., & Wang, Z. (2019). sEMG Signal Processing Methods : A Review. *The Electrochemical Society*. doi:10.1088/1742-6596/1237/3/032008